Earth Syst. Dynam. Discuss., 6, 1579–1604, 2015
www.earth-syst-dynam-discuss.net/6/1579/2015/
doi:10.5194/esdd-6-1579-2015

Earth System Dynamics Discussions
Open Access

Divergent predictions of carbon storage between two global land models: attribution of the causes through traceability analysis

R. Rafique[1,2], J. Xia[1], O. Hararuk[1,3], G. Asrar[2], Y. Wang[4], and Y. Luo[1]

[1]Department of Microbiology and Plant Biology, University of Oklahoma, Norman, OK, USA
[2]Joint Global Change Research Institute, Pacific Northwest National Lab, College Park, MD, USA
[3]Pacific Forestry Centre, Victoria, BC, Canada
[4]CSIRO Ocean and Atmosphere Flagship, PMB 1, Aspendale, Victoria 3195 Australia

Received: 29 July 2015 – Accepted: 12 August 2015 – Published: 27 August 2015

Correspondence to: R. Rafique (rashidbao@gmail.com) and Y. Luo (yluo@ou.edu)

Published by Copernicus Publications on behalf of the European Geosciences Union.

Abstract

Representations of the terrestrial carbon cycle in land models are becoming increasingly complex. It is crucial to develop approaches for critical assessment of the complex model properties in order to understand key factors contributing to models' performance. In this study, we applied a traceability analysis, which decomposes carbon cycle models into traceable components, to two global land models (CABLE and CLM-CASA') to diagnose the causes of their differences in simulating ecosystem carbon storage capacity. Driven with similar forcing data, the CLM-CASA' model predicted ~31 % larger carbon storage capacity than the CABLE model. Since ecosystem carbon storage capacity is a product of net primary productivity (NPP) and ecosystem residence time (τ_E), the predicted difference in the storage capacity between the two models results from differences in either NPP or τ_E or both. Our analysis showed that CLM-CASA' simulated 37 % higher NPP than CABLE due to higher rates of carboxylation (Vc_{max}) in CLM-CASA'. On the other hand, τ_E, which was a function the baseline carbon residence time (τ'_E) and environmental effect on carbon residence time, was on average 11 years longer in CABLE than CLM-CASA'. The difference in τ_E was mainly found to be caused by longer τ'_E in CABLE than CLM-CASA'. This difference in τ_E was mainly caused by longer τ'_E of woody biomass (23 vs. 14 years in CLM-CASA') and higher proportion of NPP allocated to woody biomass (23 vs. 16 %). Differences in environmental effects on carbon residence times had smaller influences on differences in ecosystem carbon storage capacities compared to differences in NPP and τ'_E. Overall; the traceability analysis is an effective method for identifying sources of variations between the two models.

1 Introduction

Terrestrial ecosystems play a central role in the global carbon cycle as both a reservoir for carbon and as a regulator of atmospheric concentrations of carbon dioxide

ESDD
6, 1579–1604, 2015

(CO_2) (Sitch et al., 2013). Future concentrations of atmospheric CO_2 strongly depend on the feedbacks between terrestrial ecosystems and atmosphere; particularly the balance of carbon uptake, driven primarily by CO_2 in simulations; and loss of carbon from the ecosystems, driven primarily by temperature in simulations (Luo, 2007; Luo et al., 2009a; Thornton et al., 2009). Improving our understanding of the processes by which ecosystems interact with the atmosphere is of fundamental importance for improving models' predictions (Zhou et al., 2012). The global land models are the major tools for investigating the climate impacts on terrestrial ecosystem carbon storage capacity (Luo et al., 2012). Today's land models have become very sophisticated due to inclusion of multitude of different processes in the hope of simulating the real world more accurately. However, the addition of new processes not only increases the challenge of understanding the complex model behavior but also hinders the diagnosis of uncertainty in model outputs (Luo et al., 2009b; Xia et al., 2013).

Many studies have been conducted on evaluation and intercomparison of carbon cycle components of Earth System Models (Johns et al., 2011; Taylor et al., 2011; Zaehle et al., 2014), and most of these studies show large discrepancies in modeled carbon stocks and fluxes. For example, the Coupled Model Intercomparison Project (C4MIP) reported that carbon uptake responses to a doubling of atmospheric CO_2 concentrations varied from 100 to 800 Gt carbons amongst 11 models for a period of 1850–2100 years (Friedlingstein et al., 2006; Arora et al., 2011). Similarly, Todd-Brown et al. (2013) reported that the present day total soil organic carbon simulated by CMIP5 models varied six fold ranging from approximately 510 to 3040 Pg of carbon. Most of these studies use a conventional approach for model intercomparison where models are analyzed by comparing their outputs among each other and with reference data set; however this approach is not sufficient for understanding the causes of discrepancies in model outputs.

There have been a few studies that attempt explaining some of these differences in model outputs by attributing sources of variations. For example, Mishra et al. (2013) identified uncertainties in modeling soil carbon in permafrost regions but insufficiently

ESDD
6, 1579–1604, 2015

attributed these variations to different components of their model due to lack of comprehensive tractable approach. Wang et al. (2011) decomposed ecosystem models into several components, such as climate forcing, net primary productivity (NPP) allocation and decomposition rates. This study was partly successful in diagnosing uncertainties in simulated carbon dynamics. However, the framework they used could not adequately address the sources of variations to their origins thoroughly. For example, this framework was not sufficient to explain the variations in respirational fluxes (i.e. whether they were caused by carbon pool sizes or turnover rates). Similarly, Todd-Brown et al. (2013, 2014) explained the model differences based on the variations in NPP, bulk soil decomposition rates and temperature sensitivity. However, they did not describe the effects of parameterizations such as NPP partitioning, carbon transfer coefficients and decomposition rates of individual pools. These shortcomings can only be addressed after gaining more complete understanding of the model's fundamental structural differences and its traceable components controlling the carbon dynamics.

The traceability framework developed by Xia et al. (2013) provides a powerful method for attributing the sources of variations to different components of models. This framework is based on fundamental properties of the carbon cycle, which can be decomposed into few traceable components (Luo et al., 2003; Luo and Weng, 2011). After carbon is fixed by photosynthesis, its further fate can be summarized by ecosystem carbon residence time, which is a length of time a carbon atom spends in ecosystem before leaving it via respiration (Luo et al., 2001). The framework traces modeled ecosystem carbon storage capacity ($\boldsymbol{X}_{ss}$) to (i) a product of NPP and ecosystem residence time (τ_E). The latter ecosystem residence time can be further traced to (ii) baseline carbon residence times (τ_E'), which are usually preset in a model according to vegetation characteristics and soil types, (iii) environmental scalars (ξ) including temperature and water scalars, and (iv) the external climate forcing.

In this study we applied the traceability framework to decompose two commonly used complex land models (CLM-CASA' and CABLE) at global and biome spatial scales into traceable components for better understanding of the sources of variations in modeled

ESDD
6, 1579–1604, 2015

carbon storage capacity. The specific objectives of this study were to (1) quantify the effects of NPP and ecosystem residence time in determining the ecosystem carbon storage, (2) identify the influence of NPP partitioning and carbon transfer coefficients in determining baseline carbon residence time and (3) study the effects of environmental scalars and climate forcing on ecosystem residence time.

2 Methods

2.1 CABLE and CLM-CASA' models

CABLE is an Australian land model used for the simulation of land atmospheric exchanges (Kowalczyk et al., 2006). The biogeochemical model in CABLE is adopted from CASACNP, a model developed by Wang et al. (2010). CASACNP consists of tightly coupled carbon, nitrogen and phosphorus cycles. Like most of other land models, CABLE's carbon cycle also consists of typical pool and flux structure. There are nine carbon pools in the CABLE model: three plant pools, three litter pools and three soil pools. The carbon partitioning of photosynthetically fixed carbon into plant pools is controlled by the availability of light, water and nitrogen. The carbon transfer among pools is determined by the lignin/nitrogen ratio and the lignin fraction. The potential decay rates vary with vegetation types, lignin fraction and soil texture. The environmental scalar regulates the leaf turnover rates via limitations of soil moisture and soil temperature conditions. The more detailed description of CABLE model is given in Wang et al. (2011) and Xia et al. (2013).

CLM-CASA' model combines the biogeophysics of the CLM with Carnegie–Ames–Stanford Approach (CASA) biogeochemistry module (Oleson et al., 2008). The CLM released in 2008, is a component of the Community Climate System Model (CCSM) (Oleson et al., 2007). CLM examines the physical, chemical, and biological processes through which terrestrial ecosystems interact with climate. CASA' simulates carbon dynamics at the plant functional type (PFT) level beginning with carbon assimilation

ESDD
6, 1579–1604, 2015

via photosynthesis, to mortality and decomposition, and the release of CO_2 to the atmosphere. There are three plant carbon pools, six litter pools and three soil pools. A more detailed description of the model is provided by Doney et al. (2006).

Biomes for both CABLE and CLM-CASA' were constructed from the 1 km International Geosphere–Biosphere Program Data and Information System (IGBP DISCover) dataset (Loveland et al., 2000). In CLM-CASA', however, the above dataset was combined with 1 km University of Maryland tree cover dataset (DeFries et al., 2000). The CABLE model has 9 biomes (8 used in this study), and CLM-CASA' has 16 plant functional types. We aggregated the CLM-CASA' output from plant functional types to the scale of biomes as defined in CABLE. Furthermore, the photosynthetic parameters, rate of carboxylation (Vcmax) and specific leaf areas (SLA) were taken from the input files included in models' packages. The preset value of Q10 in CABLE was 1.72 (Zhou et al., 2009), 14 % lower than the Q10 value used in CLM-CASA'.

2.2 Mathematical description of carbon cycle and traceability framework

The carbon cycle in most models share four common properties: (1) photosynthesis as the starting point of carbon flow in an ecosystem, (2) partitioning of assimilated carbon into different vegetation components, (3) carbon transfer is controlled by donor pool, and, (4) first order decay of litter and soil organic matter. These fundamental properties of the terrestrial carbon cycle can be described using following equation (Luo et al., 2003; Luo and Weng, 2011).

$$\frac{\mathrm{d}\boldsymbol{X}(t)}{\mathrm{d}t} = \boldsymbol{B}U(t) - \mathbf{A}(\boldsymbol{\xi}(E)\mathbf{C})\boldsymbol{X}(t) \quad (1)$$

Where, $\boldsymbol{X}(t) = (\boldsymbol{X}_1(t), \boldsymbol{X}_2(t), \ldots, \boldsymbol{X}_n(t))^T$ is a vector of length n. $\boldsymbol{B}$ is an $n \times 1$ vector representing the partitioning coefficients of the photosynthetically fixed carbon into plant pools. $U(t)$ is the photosynthetically fixed carbon (NPP). $\mathbf{A}$ is an $n \times n$ matrix representing the carbon transfer between pools. $\boldsymbol{\xi}(E)$ is an $n \times n$ diagonal matrix of environmental scalars representing the effects temperature and moisture on decomposition rates. $\mathbf{C}$

ESDD
6, 1579–1604, 2015

is an $n \times n$ diagonal matrix representing the exit rates of carbon left in pool at each time step.

The mutually independent properties of all these elements ($\boldsymbol{B}, \mathbf{A}, \mathbf{C}$ and $\boldsymbol{\xi}(E)$) enable us to implement the analytical framework by decomposing the total ecosystem carbon storage capacity into its traceable components as described in Xia et al. (2013). The elements in $\boldsymbol{\xi}(E)$ and $U(t)$ in Eq. (1) vary with time and climatic conditions, but their long-term averages can be used to calculate steady state carbon pool sizes, $\boldsymbol{X}_{ss}$, by letting Eq. (1) equal zero for a given U_{ss} and $\boldsymbol{\xi}_{ss}$, as described in Xia et al. (2013):

$$\boldsymbol{X}_{ss} = [\mathbf{A}\boldsymbol{\xi}_{ss}\mathbf{C})]^{-1}\boldsymbol{B}U_{ss} \quad (2)$$

The vector $\boldsymbol{X}_{ss}$ represents the steady state carbon pools. U_{ss} is the steady state carbon influx in an ecosystem. The partitioning ($\boldsymbol{B}$), transfer coefficients and exit rates ($\mathbf{A}$ and $\mathbf{C}$) in Eq. (2) together determine the baseline carbon residence time (τ'_E):

$$\tau'_E = (\mathbf{AC})^{-1}\boldsymbol{B} \quad (3)$$

The baseline carbon residence time (τ'_E) in Eq. (3) and environmental scalar values describe the total ecosystem residence time (τ_E):

$$\tau_E = \boldsymbol{\xi}_{ss}^{-1}\tau'_E \quad (4)$$

Thus the ecosystem carbon storage capacity is jointly determined by the ecosystem residence time (τ_E) and steady state carbon influx (U_{ss}):

$$\boldsymbol{X}_{ss} = \tau_E U_{ss} \quad (5)$$

Equation (5) also defines the total ecosystem residence time as the ratio of carbon storage ($\boldsymbol{X}_{ss}$) to steady state carbon influx (U_{ss}) ($\tau_E = \boldsymbol{X}_{ss}/U_{ss}$)

The environmental scalar is further separated into the temperature ($\boldsymbol{\xi}_T$) and water ($\boldsymbol{\xi}_W$) scalar components which can be represented as:

$$\boldsymbol{\xi}_{ss} = \boldsymbol{\xi}_W\boldsymbol{\xi}_T \quad (6)$$

ESDD
6, 1579–1604, 2015

The set of Eqs. (2–6) not only decomposes the carbon storage capacity into different traceable components in a systematic way, but also explains the mutual relationships among them. The additional information on the description of traceability components can be found at http://ecolab.ou.edu/?research_info&id=36.

2.3 Model simulations and diagnosis

Modeled carbon dynamics heavily depends on the initial conditions of state variables (carbon pools), which, in Earth System Models, are customarily assumed to be steady state pools (in the year 1850). In this study, for the estimation of modeled carbon storage capacity and other traceable components, the steady state of the models was obtained through spin up simulations. The process of spin up was carried out using the semi analytical solution (SAS) method developed by Xia et al. (2012). For spin up, the models were simulated until the mean changes in carbon pools over each loop (1 year) were smaller than 0.01 % year^{-1} in each cycle. The CLM-CASA and CABLE models were forced with the climate forcing data reported in Qian et al. (2006) and Wang et al. (2010), respectively. The CO_2 concentration was set at 375 ppm for both models' runs. Inputs for soil texture in both models were taken from IGBP-DIS dataset (IGBP-DIS, 2000). For both models, the lignin content and CN ratios were assigned for each plant functional type in the source code (therefore there was no map of them) and lignin to nitrogen ratios were calculated from PFT-level CN ratios and lignin content. The models were run on two spatial resolutions of $2.81^\circ \times 2.81^\circ$ (CLM-CASA') and $1^\circ \times 1^\circ$ (CABLE). After the spin up simulations, elements of **A**, **C**, ***B***, and $\boldsymbol{\xi}$**(E)**, *as well as* $U(t)$ were stored to calculate their mean values. The obtained averages were used to calculate the carbon residence time and steady state carbon pools (Eqs. 2–4).

ESDD
6, 1579–1604, 2015

3 Results

3.1 Carbon storage in CABLE and CLM-CASA'

The ecosystem carbon storage capacity, jointly determined by ecosystem residence time and carbon influx, differed substantially between CABLE and CLM-CASA' at both global and biome levels. CLM-CASA' had 31 % higher global carbon storage capacity compared to CABLE (Circled in Fig. 1). In both models, evergreen needleleaf forest and evergreen broadleaf forest showed the highest carbon storage capacity. However, evergreen needleleaf forest and evergreen broadleaf forest in CLM-CASA' had 63 and 47 % higher carbon storage capacity compared to respective biomes in CABLE. Shrub land, C3G and C4G showed the most agreement between two models. In general, the biomes with higher carbon storage capacity of both models, showed moderate NPP and higher ecosystem residence times.

A substantial variation was observed in the simulated NPP and estimated ecosystem residence time at both global and biomes level between CABLE and CLM-CASA'. All biomes in CLM-CASA' produced higher NPP compared to the respective biomes in CABLE. Three biomes, evergreen broadleaf forest, C4G and deciduous broadleaf forest in CLM-CASA' produced NPP higher than 1000 $g\,C\,m^{-2}\,yr^{-1}$ compared to one biome (evergreen broadleaf forest) of same value in CABLE (Fig. 1). The minimum value of NPP (250 $g\,C\,m^{-2}\,yr^{-1}$ for deciduous needleleaf forest) in CLM-CASA' was much higher than the minimum value of NPP (61 $g\,C\,m^{-2}\,yr^{-1}$ for tundra) in CABLE. The similar diverse trend was also observed for the ecosystem residence time at global and biome levels between CABLE and CLM-CASA'. In CLM-CASA', three biomes (deciduous needleleaf forest, evergreen needleleaf forest and tundra) showed ecosystem residence time of $>$ 100 years compared to two biomes (deciduous needleleaf forest and tundra) in CABLE. However, C4G in both models had represented the shortest ecosystem residence time in CLM-CASA' (13 years) and CABLE (18 years).

ESDD
6, 1579–1604, 2015

3.2 Baseline carbon residence time and its components

Baseline carbon residence time along with the environmental scalar plays an important role in determining the total ecosystem carbon residence time (Eq. 5). Both CABLE and CLM-CASA' showed large variations in baseline carbon residence times at both global and biome levels (Fig. 2). The global baseline residence time of 20 years in CABLE was approximately five fold higher than the global baseline carbon residence time of CLM-CASA'. The deciduous needleleaf forest and evergreen needleleaf forest in both models showed the highest baseline carbon residence times amongst biomes. However, the deciduous needleleaf forest and evergreen needleleaf forest in CABLE showed 79 and 82 % higher baseline carbon residence times compared to respective biomes in CLM-CASA'. The tundra in CABLE showed the minimum baseline carbon residence time, whereas, it was ranked third highest in CLM-CASA'. Similarly, the baseline carbon residence time of shrub land in CABLE was 89 % higher than the baseline carbon residence time of tundra in CLM-CASA'. In general, five biomes (evergreen needleleaf forest, evergreen broadleaf forest, deciduous needleleaf forest, deciduous broadleaf forest, shrub land) in CABLE showed baseline residence time > 15 years compared to the maximum baseline carbon residence time of 9 years for deciduous needleleaf forest in CLM-CASA'.

The baseline carbon residence time is dependent on NPP partitioning coefficients (vector $\boldsymbol{B}$), carbon transfer coefficients (matrix **A**) and decomposition rates (matrix **C**) (Eq. 4). All these components of $\boldsymbol{B}$, **A**, and **C** showed substantial differences between the two models. CABLE allocated 61 % of NPP to roots, 23 % to wood and 16 % to leaves (Fig. 3a). CLM-CASA' allocated 43 % of NPP to leaves, 16 % to wood and 41 % to roots (Fig. 3b). Similarly, a large difference in carbon transfers from live plants to litter and soil was also observed. In CABLE, the live tissues were partitioned into three litter pools (including CWD). 59 % of leaf carbon partitioned to metabolic litter and 41 % to structural litter pools, while roots transferred 61 % of their carbon to metabolic and 39 % to structural litter. A major portion of litter carbon was released into the atmosphere

ESDD
6, 1579–1604, 2015

through respiration losses, while the remaining was transferred into the soil organic matter pools (Fig. 3a). In CLM-CASA', the plant tissues dispersed to six litter pools (including CWD) after mortality. The leaves allocated 62 % of its carbon to surface metabolic litter and 38 % to surface structural litter. Likewise, the fine roots allocated 62 % of its carbon to soil metabolic litter and 38 % to soil structural litter. All of the litter pools contributed to three soil carbon pools which were then interlinked for back and forth movement of carbon until it was respired completely (Fig. 3b). CLM-CASA' and CABLE also differed in representing their **C** matrix which was a fraction of carbon leaving from each pool with values in CLM-CASA' being higher than in CABLE, in general.

3.3 Photosynthetic parameters

The magnitude of NPP is one of the two factors that control ecosystem carbon storage capacity in CLM-CASA' and CABLE. Differences in NPP between the two models could've been caused by differences in model forcing, or in model parameterization of photosynthesis process. As illustrated in Fig. 4, there were no significant differences in models' climatic forcing, whereas, photosynthetic parameters differed substantially. For most biomes CLM-CASA' had higher Vcmax and SLA values (Table 1), which caused the NPP to be higher than in CABLE.

3.4 Climate forcing

Environmental forcing (air temperature and precipitation), a determinant of environmental scalars, plays a considerable role in regulating the ecosystem residence time through controlling the decomposition rates. The mean air temperature ($11.2 \pm 4.9\,^{\circ}C$) and precipitation (973 ± 457 mm) in CABLE was comparable to mean air temperature ($11.7 \pm 5.1\,^{\circ}C$) and precipitation (967 ± 490 mm) in CLM-CASA' (Fig. 4). A strong agreement between climate forcing was also observed between the biomes of both models. However, a few biomes showed more substantial variations in climate forcing between

ESDD
6, 1579–1604, 2015

CABLE and CLM-CASA'. The maximum difference between mean air temperatures of both models was observed for deciduous broad leaf forest followed by tundra and deciduous needleleaf forest, respectively (Fig. 4). CLM-CASA' showed 18 % higher mean air temperature for deciduous broad leaf forest compared to CABLE. In both models, tundra (−8.0 ± 5.2 °C in CABLE; −5.5 ± 5.2 °C in CLM-CASA') and deciduous needleleaf forest (−7.0 ± 1.4 °C in CABLE; −9.8 ± 1.2 °C in CLM-CASA') showed much lower air temperature compared to all other biomes. The variation in climate forcing of two models was relatively more pronounced in precipitation data compared to air temperature data. The maximum differences in precipitation data between both models were found in C4G, tundra and deciduous needleleaf forest respectively. In CABLE, C4G (1018 ± 491 mm) presented 59 % lower precipitation compared to C4G (1622 ± 765 mm) in CLM-CASA'. However, CABLE exhibited 46 and 43 % more precipitation for tundra and deciduous needleleaf forest compared to that of respective biomes in CLM-CASA'. Deciduous broad leaf forest, shrub land, and C3G in both models showed similar precipitation data in both models.

3.5 Environmental scalars

The environmental scalars at global and biomes levels differed substantially between two models (Fig. 5). The global average of environmental scalar in CABLE (0.34) was considerably lower compared to that of CLM-CASA' (0.42). In general, CLM-CASA' simulated higher environmental scalar values for most of the biomes compared to CABLE. C4G, shrub land and evergreen broadleaf forest were least limited by temperature and moisture with environmental scalars of 0.65 and 0.49, respectively. Both models simulated tundra with the highest temperature and moisture limitation of organic matter decomposition.

The environmental scalar is jointly determined by temperature and water scalars. The global temperature and water scalars in CLM-CASA' were found to be 16 and 4 % higher than that of CABLE. The temperature scalars were strongly dependent on the Q10 value, which was 14 % higher in CLM-CASA' than in CABLE. The C4G

ESDD
6, 1579–1604, 2015

and evergreen broadleaf forest in CABLE and evergreen broadleaf forest and deciduous broadleaf forest in CLM-CASA', showed the highest temperature scalar values amongst all other biomes (Fig. 5). The minimum temperature scalar was observed for tundra in CABLE and deciduous needleleaf forest in CLM-CASA'. Overall, organic matter decomposition (across the biomes) in CABLE was more dependent on temperature than the organic matter decomposition in CLM-CASA'. The same diverse pattern of biome level water scalars was observed in both models (Fig. 5). The deciduous needleleaf forest (0.87) in CABLE and C4G (0.86) in CLM-CASA' showed the maximum water scalar values. Similarly, evergreen broad leaf forest (0.65) in CABLE and tundra (0.16) in CLM-CASA' showed the minimum environmental scalar values. In general, CLM-CASA' presented higher values of water scalars for most of biomes compared to CABLE. Furthermore, environmental scalars were mainly determined by temperature rather than water scalar in both models.

4 Discussion

The traceability framework implemented in this study is an effective method to characterize the major components of the carbon cycle represented by two widely used land models, CABLE and CLM-CASA'. We were able to identify the differences in modeled carbon storage capacity in an independent manner through decomposing of the carbon cycle into its major components of NPP, ecosystem residence time and environmental scalars (Eqs. 1–6). For example, the global carbon storage capacity in CLM-CASA' was substantially higher (31 %) compared to that in CABLE, primarily due to 37 % higher simulated NPP slightly offset by lower ecosystem residence time (Figs. 1 and 6). The higher NPP in CLM-CASA' was attributed to the relatively higher rates of carboxylation and specific leaf areas (Table 1) compared to CABLE. Longer ecosystem residence time in CABLE was mainly attributed to higher environmental limitation of the organic matter decomposition.

ESDD
6, 1579–1604, 2015

Both models showed a distinctive pattern of NPP partitioning and transferring carbon among different pools (Fig. 3) which resulted in different baseline carbon residence times. The baseline carbon residence time in CABLE was longer due to more NPP partitioning into roots and wood, which had higher residence times than in CLM-CASA'. Previous studies also reported that partitioning of NPP among different pools is a significant factor in determining carbon residence time (Todd-Brown et al., 2013; Rafique et al., 2014). In CABLE, the allocation of NPP into plant pools was mainly driven by the availability of water, nitrogen and light (Xia et al., 2013), whereas, CLM-CASA' considers only water and light (Friedlingstein et al., 1999). CABLE and CLM-CASA' also differed significantly in transferring carbon among pools, and their corresponding respiration loss (Fig. 3). The most obvious difference was the pattern of carbon transfer from live tissues to litter pools. These carbon transfer rates among pools directly influence the carbon pool sizes and residence time (Xia et al., 2013).

Environmental scalars strongly influenced the actual ecosystem residence time and varied substantially across the biomes in both models. Temperature scalars in both models showed more diverse distribution than water scalars, indicating that temperature limitation was more important in determining actual ecosystem residence time than water limitation (Todd-Brown et al., 2014). However, water scalars were more variable across biomes in CLM-CASA' than in CABLE. Despite the similarity of air temperature data used in both models (Fig. 4), the temperature scalars were found to be different between the two models due to the considerable difference in Q10 value, which was higher in CLM-CASA'.

The traceability framework is an effective method for explaining the models variations, a major issue identified by previous studies (Friedlingstein et al., 2006; Wang et al., 2011; Mishra et al., 2013; Todd-Brown et al., 2013; Rafique et al., 2014; Zaehle et al., 2014). Overall, our results showed that the major factors contributing to the differences between the two models were due to parameter settings related to photosynthesis, carbon input, baseline residence times and Q10 values. This study provides information on the relative importance of model components and source of variations

ESDD
6, 1579–1604, 2015

which are useful for model intercomparisons, benchmark analyses and evaluation of additional components in models. Hence, this framework can be applied to other biogeochemical models to better characterize and quantify the processes that contribute to model differences. For example, CLM4, VEGAS and CENTURY share similar structure of carbon cycle modules and thus can be diagnosed through the traceability framework for evaluating the models' performance.

5 Summary

The modeled total carbon storage capacity in CLM-CASA' was ~31 % higher compared to CABLE, due to the combined effect of higher NPP and lower ecosystem residence time. At biome level, evergreen needle-leaf forest and evergreen broadleaf forests in CLM-CASA' showed 63 and 47 % higher carbon storage capacity as compared to similar biomes simulated by CABLE. The ecosystem residence time was primarily dependent on the baseline carbon residence time and environmental scalar. Both CABLE and CLM-CASA' showed large variations in baseline carbon residence times, which is largely influenced by parameters of NPP partitioning coefficients (vector ***B***), carbon transfer coefficients (matrix **A**) and decomposition rates (matrix **C**). All these components of ***B***, **A** and **C** showed substantial difference in both models and consequently influenced the overall carbon storage capacity.

The global average of environmental scalar in CABLE (0.34) was lower compared to that of CLM-CASA' (0.42). At biome level, CLM-CASA' exhibited higher environmental scalar values for most of the biomes compared to respective biomes in CABLE. The difference in environmental scalars between CABLE and CLM-CASA' was largely due to the differences in temperature scalars rather than water scalars. Overall, our results suggested that the differences in carbon storage between the two models were largely influenced by parameter settings related to photosynthesis, baseline residence times and temperature limitation of organic matter decomposition. The different NPP values were determined by the differences in Vcmax and SLA, while the differences in baseline

ESDD
6, 1579–1604, 2015

carbon residence times were determined by differences in NPP partitioning and carbon transfer coefficients.

Acknowledgements. This work is financially supported by USA Department of Energy, Terrestrial Ecosystem Sciences grant DE SC0008270 and National Science Foundation (NSF) grant DEB 0743778, DEB 0840964, EPS 0919466, and EF 1137293. Partial support for final preparation of this paper was provided by a Laboratory Directed Research and Development grant by the Pacific Northwest national Laboratory of the US Department of Energy. The data produced and used in this study can be obtained on request from Yiqi Luo (Email: yluo@ou.edu). However, the source codes for the CABLE and CLM-CASA are located at https://trac.nci.org.au/trac/cable/wiki and http://www.cgd.ucar.edu/tss/clm/distribution/clm3.5, respectively. We are thankful to Lifen Jiang, Katherine Todd-Brown, Xia Xu, Zheng Shi, Junyi Liang and Changting Wang for their suggestions and feedback in conducting this research.

References

Arora, V. K., Scinocca, J. F., Boer, G. J., Christian, J. R., Denman, K. L., Flato, G. M., Kharin, V. V., Lee, W. G., and Merryfield, W. J.: Carbon emission limits required to satisfy future representative concentration pathways of greenhouse gases, Geophys. Res. Lett., 38, L05805, doi:10.1029/2010GL046270, 2011.

DeFries, R. S., M. C. Hansen, J. R. G. Townshend, A. C. Janetos, and Loveland, T. R.: A new global 1 km dataset of percentage tree cover derived from remote sensing, Glob. Change Biol., 6, 247–254, 2000.

Doney, S. C., Lindsay, K., Fung, I., and John, J.: Natural variability in a stable, 1000 yr global coupled climate–carbon cycle simulation, J. Climate, 19, 3033–3054, 2006.

Friedlingstein, P., Joel, G., Field, C. B., and Fung, I. Y.: Toward an allocation scheme for global terrestrial carbon models, Glob. Change Biol., 5, 755–770, 1999.

Friedlingstein, P., Cox, P., Betts, R., Bopp, L., von Bloh, W., Brovkin, V., Cadule, P., Doney, S., Eby, M., Fung, I., Bala, G., John, J., Jones, C., Joos, F., Kato, T., Kawamiya, M., Knorr, W. Lindsay, K., Matthews, H. D., Raddatz, T., Rayner, P., Reick, C., Roeckner, E., Schnitzler, K.-G., Schnur, R., Strassmann, K., Weaver, A. J., Yoshikawa, C., and Zeng, N.: Climate–carbon cycle feedback analysis: results from the C4MIP model intercomparison, J. Climate, 19, 3337–3353, 2006.

ESDD
6, 1579–1604, 2015

Global Soil Data Task: Global soil data products CD-ROM (IGBP-DIS), International Geosphere–Biosphere Programme – Data and Information Available Services, available at: http://www.daac.ornl.gov (last access: 15 September 2012), 2000.

Johns, T. C., Royer, J. F., Höschel, I., Huebener, H., Roeckner, E., Manzini, E., May, W., Dufresne, J.-L., Ottera, O. H., van Vuuren, D. P., Salas y Melia, D., Giorgetta, M. A., Denvil, S., Yang, S., Fogli, P. G., Körper, J., Tjiputra, J. F., Stehfest, E., and Hewitt, C. D.: Climate change under aggressive mitigation: the ENSEMBLES multi-model experiment, Clim. Dynam., 37, 1975–2003, 2011.

Kowalczyk, E. A., Wang, Y. P., Law, R. M., Davies, H. L., McGregor, J. L., and Abramowitz, G.: The CSIRO atmosphere biosphere land exchange (CABLE) model for use in climate models and as an offline model, available at: http://www.cawcr.gov.au/projects/access/cable/cable_technical_description.pdf (last access: 20 March 2013), 2006.

Loveland, T. R., Reed, B. C., Brown, J. F., Ohlen, D. O., Zhu, Z., Yang, L., and Merchant, J. W.: Development of a global land cover characteristics database and IGBP DISCover from 1 km AVHRR data, Int. J. Remote Sens., 21, 1303–1330, 2000.

Luo, Y.: Terrestrial carbon–cycle feedback to climate warming, Annu. Rev. Ecol. Evol. S., 38, 683–712, 2007.

Luo, Y. and Weng, E.: Dynamic disequilibrium of the terrestrial carbon cycle under global change, Trends Ecol. Evol., 26, 96–104, 2011.

Luo, Y., White, L. W., Canadell, J. G., DeLucia, E. H., Ellsworth, D. S., Finzi, A., Lichter, J., and Schlesinger, W. H.: Sustainability of terrestrial carbon sequestration: A case study in Duke Forest with inversion approach, Global Biogeochem. Cy., 17, 1021, doi:10.1029/2002GB001923, 2001.

Luo, Y., Sherry, R., Zhou, X., and Wan, S.: Terrestrial carbon-cycle feedback to climate warming: experimental evidence on plant regulation and impacts of biofuel feedstock harvest, Global Change Biol. Bioenerg., 1, 62–74, 2009a.

Luo, Y., Weng, E., Wu, X., Gao, C., Zhou, X., and Zhang, L.: Parameter identifiability, constraint, and equifinality in data assimilation with ecosystem models, Ecol. Appl., 19, 571–574, 2009b.

Luo, Y. Q., Randerson, J. T., Abramowitz, G., Bacour, C., Blyth, E., Carvalhais, N., Ciais, P., Dalmonech, D., Fisher, J. B., Fisher, R., Friedlingstein, P., Hibbard, K., Hoffman, F., Huntzinger, D., Jones, C. D., Koven, C., Lawrence, D., Li, D. J., Mahecha, M., Niu, S. L., Norby, R., Piao, S. L., Qi, X., Peylin, P., Prentice, I. C., Riley, W., Reichstein, M., Schwalm, C.,

ESDD
6, 1579–1604, 2015

Wang, Y. P., Xia, J. Y., Zaehle, S., and Zhou, X. H.: A framework for benchmarking land models, Biogeosciences, 9, 3857–3874, doi:10.5194/bg-9-3857-2012, 2012.

Mishra, U., Jastrow, J. D., Matamala, R., Hugelius, G., Koven, C. D., Harden, J. W., Ping, C. L., Michaelson, G. J., Fan, Z., Miller, R. M., McGuire, A. D., Tarnocai, C., Kuhry, P., Riley, W. J., Schaefer, K., Schuur, E. A. G., Jorgenson, M. T., and Hinzman, L. D.: Empirical estimates to reduce modeling uncertainties of soil organic carbon in permafrost regions: a review of recent progress and remaining challenges, Environ. Res. Lett., 8, 035020, doi:10.1088/1748-9326/8/3/035020, 2013.

Oleson, K. W., Niu, G. Y., Yang, Z.-L., Lawrence, D. M., Thornton, P. E., Lawrence, P. J., Stockli, R., Dickinson, R. E., Bonan, G. B., and Levis, S.: Technical Description of the Community Land Model (CLM3.5), NCAR Technical Note, National Center for Atmospheric Research, Boulder, CO, 2007.

Oleson, K. W., Niu, G. Y., Yang, Z. L., Yang, Z.-L., Lawrence, D. M., Thornton, P. E., Lawrence, P. J., Stöckli, R., Dickinson, R. E., Bonan, G. B., Levis, S., Dai, A., and Qian, T.: Improvements to the Community Land Model and their impact on the hydrological cycle, J. Geophys. Res.-Biogeo., 113, G01021, doi:10.1029/2007JG000563, 2008.

Qian, T., Dai, A., Trenberth, K. E., and Oleson, K. W.: Simulation of global land surface conditions from 1948 to 2004. Part I: Forcing data and evaluations, J. Hydrometeorol., 7, 953–975, 2006.

Sitch, S., Friedlingstein, P., Gruber, N., Jones, S. D., Murray-Tortarolo, G., Ahlström, A., Doney, S. C., Graven, H., Heinze, C., Huntingford, C., Levis, S., Levy, P. E., Lomas, M., Poulter, B., Viovy, N., Zaehle, S., Zeng, N., Arneth, A., Bonan, G., Bopp, L., Canadell, J. G., Chevallier, F., Ciais, P., Ellis, R., Gloor, M., Peylin, P., Piao, S. L., Le Quéré, C., Smith, B., Zhu, Z., and Myneni, R.: Recent trends and drivers of regional sources and sinks of carbon dioxide, Biogeosciences, 12, 653–679, doi:10.5194/bg-12-653-2015, 2015.

Taylor, K. E., Stouffer, R. J., and Meehl, G. A.: An overview of CMIP5 and the experiment design, B. Am. Meteorol. Soc., 93, 485–498, 2011.

Thornton, P. E. and Zimmermann, N. E.: An improved canopy integration scheme for a land surface model with prognostic canopy structure, J. Climate, 20, 3902–3923, 2007.

Thornton, P. E., Doney, S. C., Lindsay, K., Moore, J. K., Mahowald, N., Randerson, J. T., Fung, I., Lamarque, J.-F., Feddema, J. J., and Lee, Y.-H.: Carbon-nitrogen interactions regulate climate-carbon cycle feedbacks: results from an atmosphere-ocean general circulation model, Biogeosciences, 6, 2099–2120, doi:10.5194/bg-6-2099-2009, 2009.

ESDD
6, 1579–1604, 2015

Todd-Brown, K. E. O., Randerson, J. T., Post, W. M., Hoffman, F. M., Tarnocai, C., Schuur, E. A. G., and Allison, S. D.: Causes of variation in soil carbon simulations from CMIP5 Earth system models and comparison with observations, Biogeosciences, 10, 1717–1736, doi:10.5194/bg-10-1717-2013, 2013.

Todd-Brown, K. E. O., Randerson, J. T., Hopkins, F., Arora, V., Hajima, T., Jones, C., Shevliakova, E., Tjiputra, J., Volodin, E., Wu, T., Zhang, Q., and Allison, S. D.: Changes in soil organic carbon storage predicted by Earth system models during the 21st century, Biogeosciences, 11, 2341–2356, doi:10.5194/bg-11-2341-2014, 2014.

Wang, Y. P., Law, R. M., and Pak, B.: A global model of carbon, nitrogen and phosphorus cycles for the terrestrial biosphere, Biogeosciences, 7, 2261–2282, doi:10.5194/bg-7-2261-2010, 2010.

Wang, Y. P., Kowalczyk, E., Leuning, R., Abramowitz, G., Raupach, M. R., Pak, B., van Gorsel, E., and Luhar, A.: Diagnosing errors in a land surface model (CABLE) in the time and frequency domains, J. Geophys. Res.-Biogeo., 116, G01034, doi:10.1029/2010JG001385, 2011.

White, L. and Luo, Y.: Estimation of carbon transfer coefficients using Duke Forest free-air CO_2 enrichment data, Appl. Math. Comput., 130, 101–120, 2002.

Xia, J. Y., Luo, Y. Q., Wang, Y. P., and Hararuk, O.: Traceable components of terrestrial carbon storage capacity in biogeochemical models, Glob. Change Biol., 19, 2104–2116, 2013.

Zaehle, S., Medlyn, B. E., De Kauwe, M. G., Walker, A. P., Dietze, M. C., Hickler, T., Luo, Y., Wang, Y.-P., El-Masri, B., Thornton, P., Jain, A., Wang, S., Warlind, D., Weng, E., Parton, W., Iversen, C. M., Gallet-Budynek, A., McCarthy, H., Finzi, A., Hanson, P. J., Prentice, I. C., Oren, R., and Norby, R. J.: Evaluation of 11 terrestrial carbon–nitrogen cycle models against observations from two temperate free-air CO_2 enrichment studies, New Phytol., 202, 803–822, 2014.

Zhou, T., Shi, P. J., Hui, D. F., and Luo, Y. Q.: Global pattern of temperature sensitivity of soil heterogeneous respiration (Q10) and its implications for carbon-climate feedback, J. Geophys. Res.-Biogeo., 114, G02016, doi:10.1029/2008JG000850, 2009.

Zhou, X. H., Zhou, T., and Luo, Y. Q.: Uncertainties in carbon residence time and NPP-driven carbon uptake in terrestrial ecosystems of the conterminous USA: a Bayesian approach, Tellus, 64, 17223, doi:10.3402/tellusb.v64i0.17223, 2012.

ESDD
6, 1579–1604, 2015

Table 1. Photosynthesis parameter values for different biomes in CLM-CASA' and CABLE. Abbreviations of biomes are given in Fig. 1.

Biomes	CLM-CASA'		CABLE		CLM-CASA minus CABLE	
	Vcmax ($\mu mol\,m^{-2}\,s^{-1}$)	SLA ($m^2\,gC^{-1}$)	Vcmax ($\mu mol\,m^{-2}\,s^{-1}$)	SLA ($m^2\,gC^{-1}$)	Vcmax ($\mu mol\,m^{-2}\,s^{-1}$)	SLA ($m^2\,gC^{-1}$)
ENF	47	0.009	40	0.018	7	−0.009
EBF	72	0.006	55	0.021	17	−0.015
DNF	51	0.024	40	0.025	11	0.001
DBF	47	0.03	60	0.025	−13	0.005
Shrubland	22	0.024	40	0.025	−18	−0.001
C3G	43	0.05	60	0.028	−17	0.022
C4G	24	0.05	10	0.028	14	0.022
Tundra	43	0.05	60	0.028	−17	0.022

ESDD
6, 1579–1604, 2015

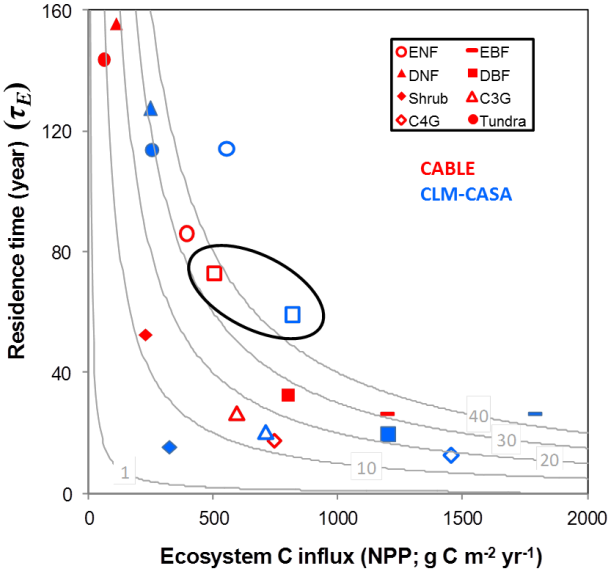

Figure 1. Determination of ecosystem carbon storage capacity (grey contour lines) by carbon in flux (U_{ss}; x axis) and ecosystem residence time (τ_E; y axis) (at global and biome levels) between CABLE and CLM-CASA'. The contour lines show the constant values of ecosystem carbon storage capacity. ENF – Evergreen needleleaf forest, EBF – Evergreen broadleaf forest, DNF – Deciduous needleleaf forest, DBF – Deciduous broadleaf forest, Shrub – Shrub land, C3G – C3 grassland, C4G – C4 grassland. Open squares in the circle show the global values.

ESDD
6, 1579–1604, 2015

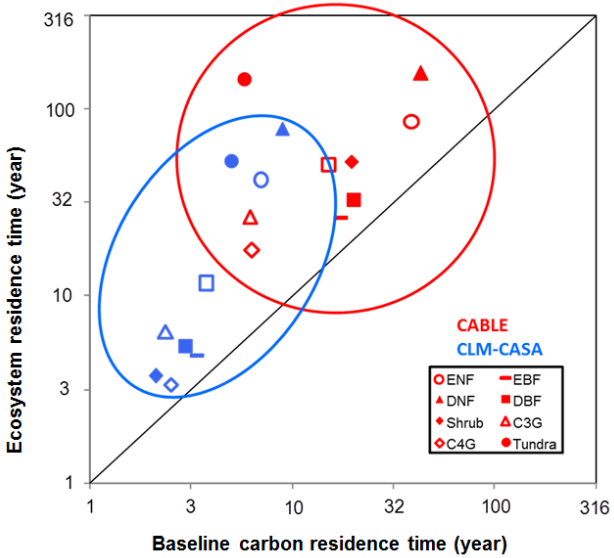

Figure 2. Spatial distribution of ecosystem residence time (τ_E) and baseline carbon residence time (τ_E') (at global and biomes level) between CABLE and CLM-CASA'. Abbreviations of biomes are given in Fig. 1. Open squares in the circle show the global values.

ESDD
6, 1579–1604, 2015

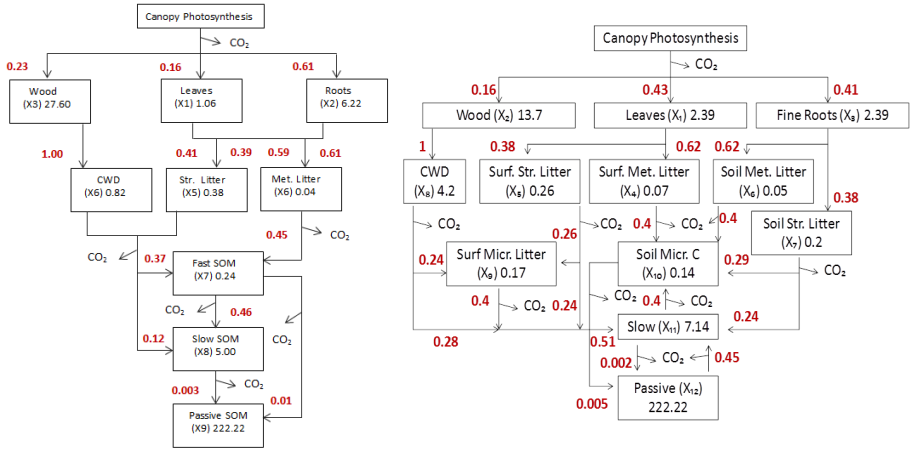

Figure 3. Schematic diagram showing the carbon cycle in CABLE (left) and CLM-CASA' (right). Carbon enters the system through photosynthesis and is partitioned among live pools. From live pools, carbon is transferred to litter pools, and from litter pools it is transferred to soil carbon pools. Values in boxes show the pools residence times. Values outside the boxes show the partitioning and transfer coefficients.

ESDD
6, 1579–1604, 2015

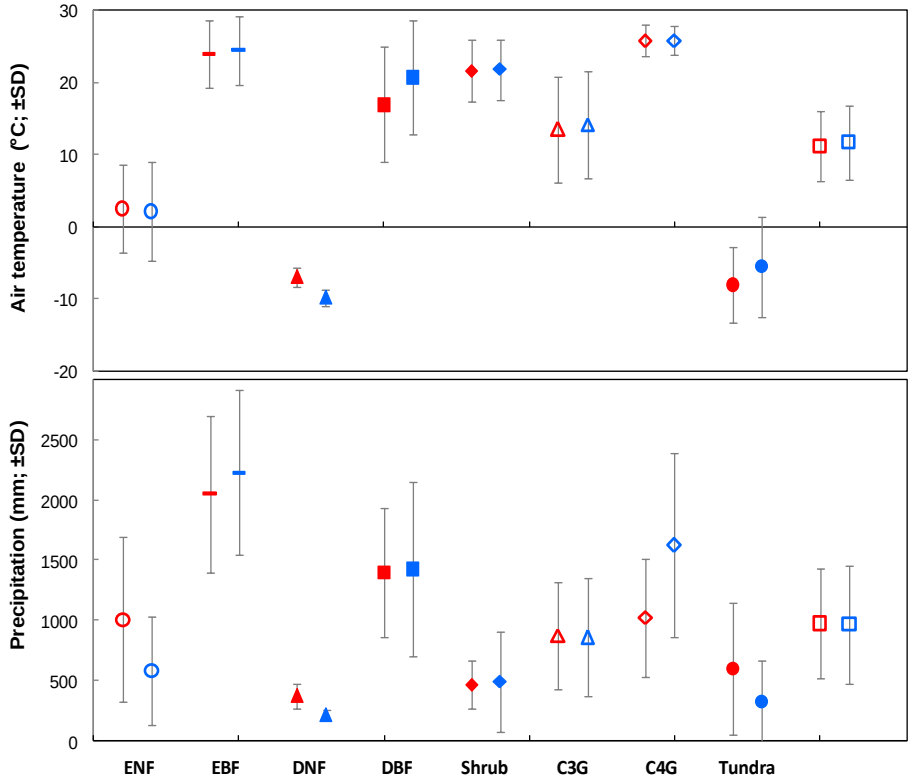

Figure 4. Distribution of climate forcing data (at global and biome levels) used for CABLE and CLM-CASA' simulations. Open square show the global values. Abbreviations of biomes are given in Fig. 1.

ESDD
6, 1579–1604, 2015

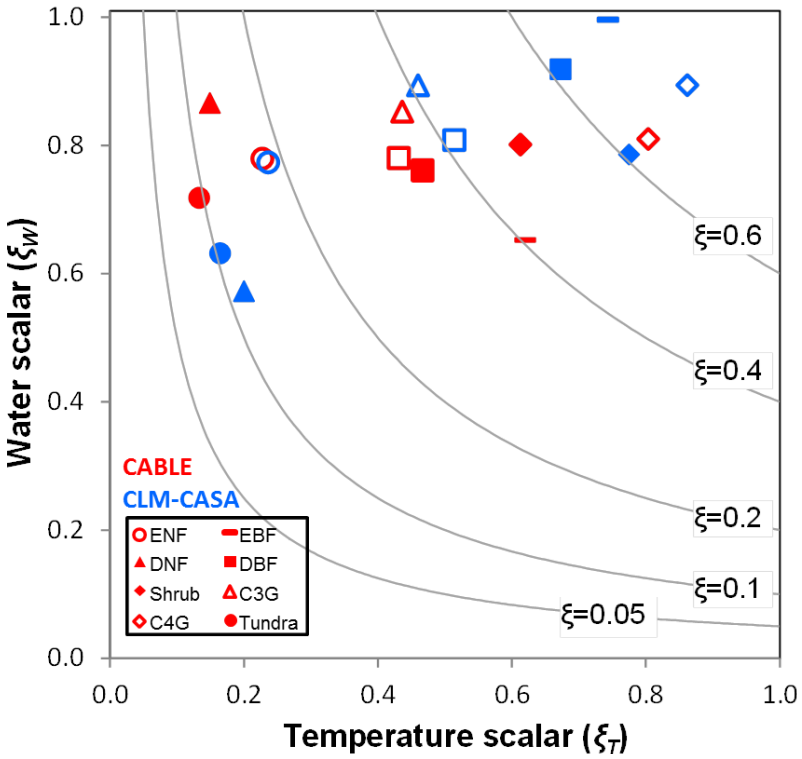

Figure 5. Determination of environmental scalars by the temperature and water scalars (at global and biome levels) between CABLE and CLM-CASA'. Open squares show the global values. The contour lines show the constant value of environmental scalars. Abbreviations of biomes are given in Fig. 1.

ESDD
6, 1579–1604, 2015

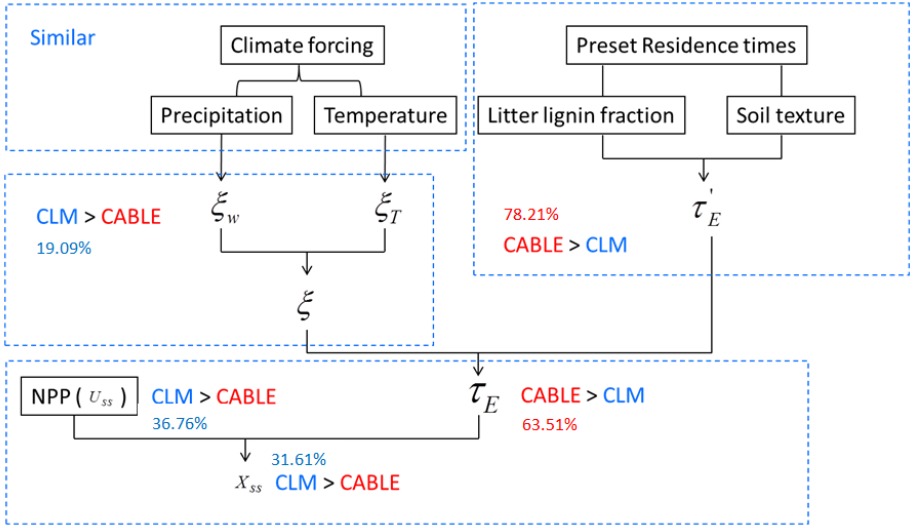

Figure 6. Schematic diagram of the traceability framework along with the summary of the results obtained in this study. The numerical values show the percentage increase between two models. $\boldsymbol{X}_{ss}$ – ecosystem carbon storage capacity; τ_E – ecosystem carbon residence time; τ_E' – baseline carbon residence time; ξ – environmental scalar; ξT – temperature scalar; ξW – water scalar.

ESDD
6, 1579–1604, 2015

Divergent predictions of carbon storage between two global land models

R. Rafique et al.